symmetry

MDPI

Article

Model Test Study on the Influence of Ground Surcharges on the Deformation of Shield Tunnels

Gang Wei [1,2], Shuming Zhang [3] and Pengfei Xiang [4,*]

[1] Department of Civil Engineering, Zhejiang University City College, Hangzhou 310015, China; weig@zucc.edu.cn
[2] College of Civil Engineering and Architecture, Zhejiang University, Hangzhou 310058, China
[3] School of Civil Engineering and Architecture, Anhui University of Science and Technology, Huainan 232001, China; 31903173@stu.zucc.edu.cn
[4] Department of Architectural Engineering, Zhejiang Tongji Vocational College of Science and Technology, Hangzhou 311200, China
* Correspondence: z20120190803@zjtongji.edu.cn; Tel.: +86-150-6871-6476

Abstract: Aiming at studying the harm caused by sudden ground loadings on existing shield tunnels, a indoor scaled model test with a geometric similarity ratio of 1:15.5 was adopted. Considering the influencing factors such as ground loading, burial depth of the shield tunnel, loading position and soil properties, tunnel convergence deformation, tunnel settlement and deep settlement of soil caused by sudden ground loadings are studied. A three-dimensional finite element simulation is carried out using the Midas software, and deep settlement of soil is calculated by a theoretical method. The purpose of this model test is to further understand the influence of ground surcharges on shield tunnel deformation. The results show that the greater the ground surcharge, the greater the settlement and vertical convergence deformation of the shield tunnel; The further away from the ground surcharge, the smaller the settlement, vertical convergence deformation and lateral convergence deformation of the tunnel. When the pile load size is constant, the greater the burial depth of the tunnel, the smaller the vertical convergence deformation and settlement of the tunnel; the maximum value of deep settlement of the soil always remains at the closest point to the ground surcharge; compared with the use of dry sand, the vertical convergence deformation and settlement of the tunnel are significantly reduced when using wet sand. Both the theoretical calculation results and the numerical simulation results are in good agreement with the indoor model test results.

Keywords: ground surcharge; shield tunnel; model test; convergent deformation; settlement; deep settlement of soil

Citation: Wei, G.; Zhang, S.; Xiang, P. Model Test Study on the Influence of Ground Surcharges on the Deformation of Shield Tunnels. *Symmetry* **2021**, *13*, 1565. https://doi.org/10.3390/sym13091565

Academic Editors: Elżbieta Szafranko, Piotr E. Srokosz and Jana Korytarova

Received: 31 July 2021
Accepted: 19 August 2021
Published: 25 August 2021

1. Introduction

Sudden ground surcharges near tunnels are an important factor threatening the safety of shield tunnel structures. Many tunnel structural damage accidents caused by sudden surcharges have occurred at home and abroad for many years [1–4]. When a sudden ground surcharge occurs around a tunnel, the ground surcharge will produce additional loads on the shield segment, which will cause a certain deformation (convergence deformation and longitudinal uneven settlement) of the segment. When the deformation is too large, the shield segment will be damaged, the gap between the segments will increase, and the connecting bolts will fail, etc. [5–9]. In order to ensure the safety of existing shield tunnel structures, it is therefore of great significance to study the deformation laws of shield tunnels under sudden ground surcharge conditions.

At present, scholars at home and abroad have done a lot of research on the influence of ground surcharges on existing shield tunnels, including full-scale model tests [10], scaled model tests [11–13], field measurements [14,15], finite element simulations [14], theoretical calculations [16–19], etc. Xian et al. [10] used a full-scale model test to study the structural bearing capacity of shield tunnels under ground surcharge conditions; Wu et al. [11] studied the influence of the burial depth of the tunnel and the position of the ground surcharge on the deformation of existing shield tunnels by using the scaled indoor model test; Huang et al. [12] studied the deformation of the tunnel structure and the change of the earth pressure around the tunnel under the action of surface overloads by using a reduced scale indoor model test; Atkinson and Pott [13] studied the stability of tunnel structure underground loads by indoor model tests, and obtained the internal force distribution of tunnel lining structures, but the deformation of these tunnel lining structures could not be determined; Based on an actual project, Ma et al. [14] analyzed the field monitoring data of tunnel convergence deformation, established a numerical calculation model, and simulated the whole process from loading before tunnel construction to unloading after construction; Based on the Tianjin Binhai Metro Line Z2 project, Lu et al. [15] analyzed the influence of different factors on tunnel deformations under surcharge loads; [16], aiming at the tunnel damage caused by eccentric ground surcharges in the tunnel neighborhood, considering the influence of eccentric ground surcharges and the force between shield lining rings, based on the modified conventional method, deduced the calculation formulas of lining confining pressure and internal force (bending moment, axial force and shear force); Yamamoto et al. [17,18] studied and analyzed the stability of one tunnel and two tunnels in cohesive soil under the action of ground surcharges, compared the results with the predicted values and obtained relevant results; According to various engineering cases, Huang et al. [19] established a model to evaluate the resilience of shield tunnels after settlement, and compared it with the measured values. Up to now, when scholars use indoor model tests to study tunnel deformations, the tunnel model is generally simplified, and the connecting bolts between tunnel segments are simply simulated by a reduction method, and no one has studied the degree of influence of convergence deformation, settlement and deep soil settlement of shield tunnels under different ground surcharge conditions [20–25]. Therefore, it is necessary to use indoor model test methods for further research.

In this paper, the indoor scaled model test method, supplemented by a three-dimensional finite element simulation and theoretical calculation method, are used to study the lateral and vertical convergence deformation, tunnel settlement and deep soil settlement of an existing shield tunnel caused by a sudden ground surcharge on the ground, and to analyze the laws that influence ground surcharge, tunnel burial depth, ground surcharge position and soil properties. At the same time, the finite element simulation results and theoretical calculation results are compared with the indoor model test results.

2. Indoor Scaled Model Test

2.1. Introduction of Test Model

In this test, a total of 23 segments of a shield tunnel were selected as the research object. The outer diameter of the shield tunnel is 6.2 m, the ring width of the segment is 1.2 m, and the segment thickness is 0.348 m, with a total length of 27.6 m. The geometric similarity ratio of indoor model test is 1:15.5.

(1) Shield tunnel model

In order to truly simulate the actual shield tunnel, the segments of the tunnel model are made of plexiglass with E = 2.06 GPa. Each ring tunnel consists of five segments with 67.5° and one segment with 22.5°, and the segments of the tunnel model are connected by bolts. The tunnel model has an outer diameter (D_0) of 0.4 m and a length of 1.78 m. See Figure 1 for the overall tunnel model.

Figure 1. Overall schematic diagram of tunnel model.

According to the second similarity theorem, the similarity constants of each physical quantity are deduced as shown in Table 1. Table 2 lists the geometric parameters and material characteristics of tunnel model. Table 3 contains the geometric parameters and material characteristics of the tunnel connecting bolts [26].

Table 1. Similarity constant of indoor model test.

Physical Quantity	Similarity Relation	Similarity Constant	Physical Quantity	Similarity Relation	Similarity Constant
Geometric dimensions	Basic quantity	15.5	Pressure	C_q	16.75
Elastic modulus	Basic quantity	16.75	Axial force	$C_N = C_E \cdot C_L^2$	4024
Strain	C_ε	1	Bending stiffness	$C_{EI} = C_L^4$	57720
Stress	C_σ	16.75	Axial stiffness	$C_{EA} = C_L^3$	3724
Displacement	C_δ	15.5	Shear stiffness	$C_{GA} = C_L^3$	3724

Table 2. Geometric parameters and material characteristics of tunnel model.

	Outer Diameter of Segment (m)	Segment Inner Diameter (m)	Segment Thickness (m)	Ring Width (m)	Elastic Modulus of Segment (MPa)	SEGMENT Poisson's Ratio
Prototype	6.200	5.504	0.348	1.200	34,500	0.2
Model	0.400	0.356	0.022	0.077	2060	0.3

Table 3. Geometric parameters and material properties of tunnel connecting bolts.

	Bolt Length (m)	Diameter of Bolt (m)	Number of Bolts	Elastic Modulus of Bolt (MPa)	Poisson's Ratio of Bolts
Prototype	0.400	0.030	17	200,000	0.30
Model	0.027	0.002	6	33,800	0.32

(2) Indoor model box

In this indoor test, the size of model box is 1.8 m × 1.8 m × 1.5 m, the width of model box is 1.8 m, which is about 4.5 D_0, and the height is 1.5 m, which is 3.75 D_0. See Figure 2 for the model box used in our indoor model tests.

Figure 2. Photo of indoor model box.

2.2. Test Soil Material

Dried sea sand was used as the soil material in this study. In order to avoid the influence of impurities in the sea sand on the test, a sieve with an aperture of 18 meshes (about 1 mm) is used to screen out the large particles in the sea sand. See Table 4 for the physical and mechanical indexes of the dry sand.

Table 4. Physical and mechanical indexes of dry sand.

Density (g)	Moisture Content (%)	Internal Friction Angle (°)	Cohesion (kPa)	Compressive Modulus (MPa)
1.495	0.23	29	0	2.89

2.3. Test Conditions

According to four test control variables, i.e., the size of ground surcharge, the burial depth of the shield tunnel (the distance from the top of tunnel to the ground), the position of ground surcharge and the physical properties of soil, nine sets of model tests were carried out to study the transverse and vertical convergence deformation, tunnel settlement and deep settlement of soil caused by sudden ground surcharges.

Table 5 lists nine groups of test conditions, in which cases 1–4 mainly measure the transverse convergence deformation of the shield tunnel and deep settlement of soil under the action of ground surcharges, while working conditions 5–9 mainly measure the vertical convergence deformation and tunnel settlement of the shield tunnel under the action of ground surcharges.

Table 5. Test conditions.

Test Number	Ground Surcharge Position	Total Thickness of Soil Layer	Tunnel Buried Depth	Sand for Test
1	Eccentricity 0 m	1.2 m	0.6 m	Dry sand
2	Eccentricity 0.2 m	1.2 m	0.6 m	Dry sand
3	Eccentricity 0.4 m	1.2 m	0.6 m	Dry sand
4	Eccentricity 0.6 m	1.2 m	0.6 m	Dry sand
5	Eccentricity 0 m	1.1 m	0.5 m	Dry sand
6	Eccentricity 0 m	1.2 m	0.6 m	Dry sand
7	Eccentricity 0 m	1.3 m	0.7 m	Dry sand
8	Eccentricity 0 m	1.4 m	0.8 m	Dry sand
9	Eccentricity 0 m	1.2 m	0.6 m	Wet sand

Because the tunnel is small, the convergence deformation can only monitor one line at a time, so the test parameters of condition 1 and condition 6 are the same. As a standard working condition, two sets of tests are conducted, which respectively test the lateral and vertical convergence of the tunnel, the tunnel settlement and the deep settlement of soil.

The layout of displacement measuring points for vertical convergence deformation and tunnel settlement of shield tunnel is shown in Figures 3 and 4. A total of five groups of measuring points are arranged. The steel rod used to fix the displacement meter in the middle of Figure 4 is fixed on the model box and is immobile, so the difference between the data of measurement point 5 and measurement point 10 is the vertical convergence value of the tunnel, and the data of measurement point 5 is the settlement value of the tunnel.

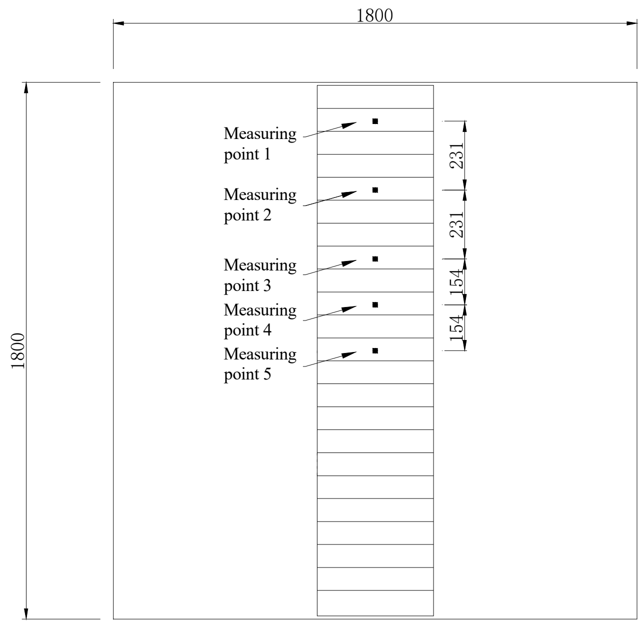

Figure 3. Layout plan of displacement meter for vertical convergence deformation of tunnel (in mm).

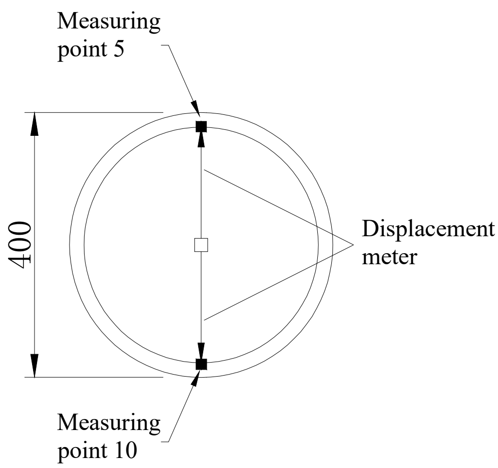

Figure 4. Layout of vertical displacement meter in tunnel (in mm).

The arrangement of displacement measuring points for transverse convergence deformation of the shield tunnel is shown in Figures 5 and 6, with a total of five groups of measuring points. The difference between the data of measuring point 15 and measuring point 20 in Figure 6 is the horizontal convergence value of the tunnel.

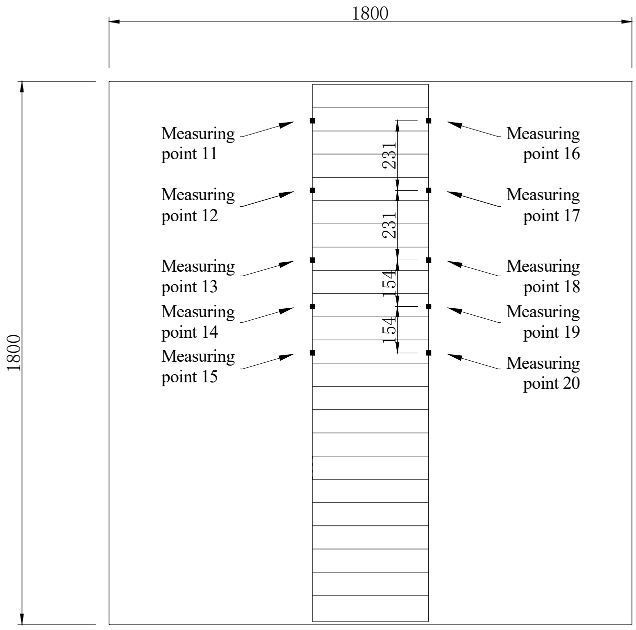

Figure 5. Layout plan of displacement meter for horizontal convergence deformation of tunnel (in mm).

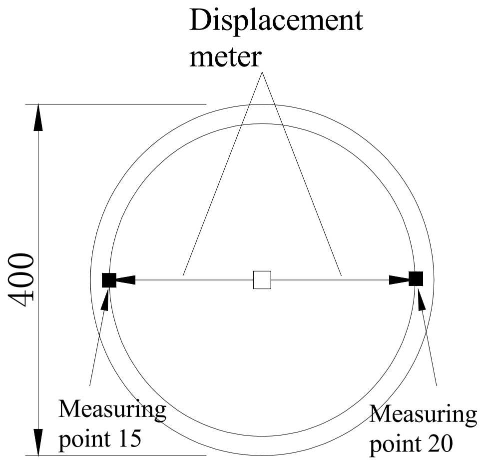

Figure 6. Layout of horizontal displacement meter in tunnel (in mm).

The arrangement of displacement measuring points for deep settlement of soil is shown in Figure 7, with a total of nine measuring points, all located 0.2 m below the ground.

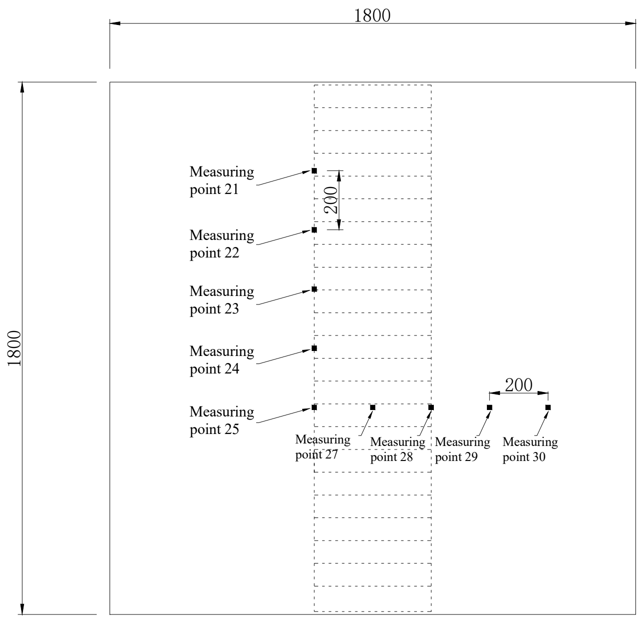

Figure 7. Layout of measuring points for deep settlement of soil (in mm).

2.4. Test Procedure

In this model test, a jack is used to press the pressure-bearing steel plate to simulate the ground surcharge. The forces exerted by the jack are 34.4, 68.8, 103.2 and 137.6 kg, respectively, and the pressure of each stage is applied at an interval of 1 h. The size of the bearing plate is 0.4 m × 0.4 m and the actual ground surcharge simulated in the test are 36, 72, 108 and 144 kPa, respectively. According to the soil gravity of 18 kN/m^3, the corresponding stacking height is 2, 4 m, 6 and 8 m, respectively, and the corresponding actual stacking range is 6.2 m × 6.2 m. The ground surcharge moves in the direction perpendicular to the shield tunnel, and the center line coincides with the center point of the shield tunnel. See Figure 8 for the model loading process.

Figure 8. Loading process of the model tests.

During the model tests, the tunnel model should be hoisted to the designated position first, and then sand should be added step by step. First, 20 cm of sand should be added to make the sand reach the bottom of the tunnel model. After standing for 24 h, the remaining height of sand should be evenly added in two times, that is, the height of the two times is the same, and each time after adding, it needs to stand for 24 h. After each group of tests, the sand in the model box is completely discharged. After that, the next group of model tests were carried out.

3. Analysis of Indoor Model Test Results

Note: The values in the analysis of test results are actually measured data.

3.1. Analysis of Test Data under Standard Operating Condition

Let the test parameters of working condition 1 and working condition 6 be the same, and the ground surcharge is just above the tunnel (symmetrical loading) as the standard working conditions. When the burial depth of the tunnel is 0.6 m and the central ground surcharge is 137.6 kg, the tunnel settlement, vertical convergence deformation, transverse convergence deformation, deep soil settlement curve (parallel to the tunnel direction) and deep soil settlement curve (perpendicular to the tunnel direction) caused by ground surcharge are shown in Figures 9–13, respectively, and the negative value in the tunnel settlement curve represents the downward settlement of the tunnel. The negative value in the vertical convergence deformation curve represents the vertical shrinkage of the tunnel; The positive value in the curve of tunnel transverse convergence deformation represents the tunnel transverse enlargement; The negative value in the deep settlement curve (including the direction parallel to and perpendicular to the tunnel) represents the decrease of soil.

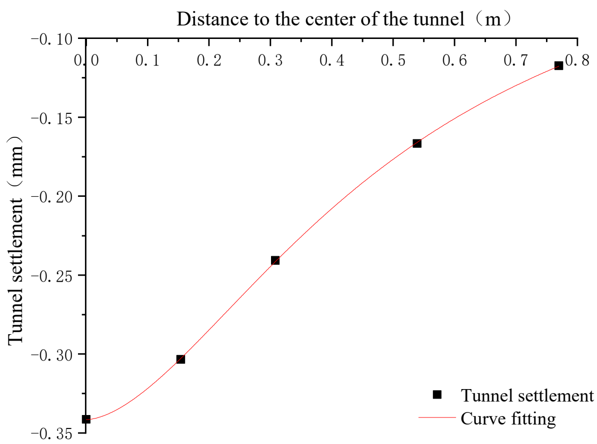

Figure 9. Tunnel settlement curve.

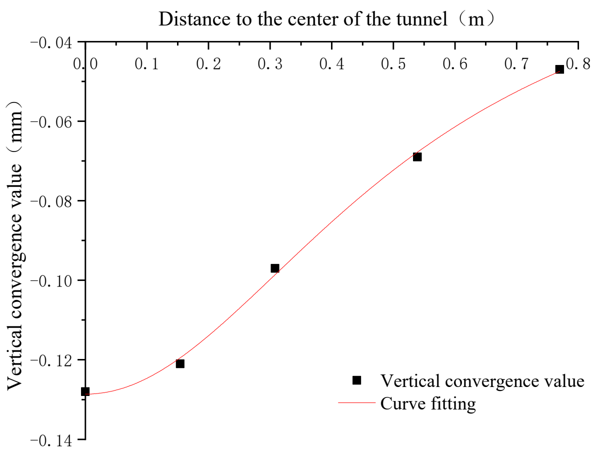

Figure 10. Vertical convergence deformation curve of tunnel.

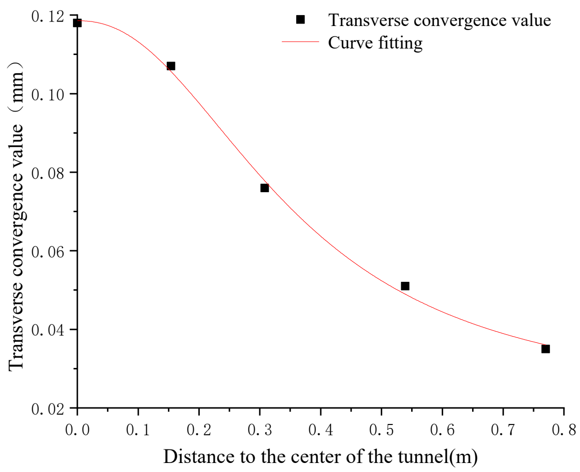

Figure 11. Transverse convergence deformation curve of tunnel.

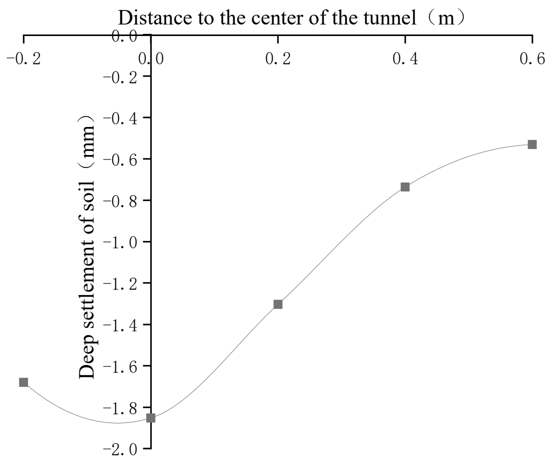

Figure 12. Deep settlement curve of soil (parallel to tunnel direction).

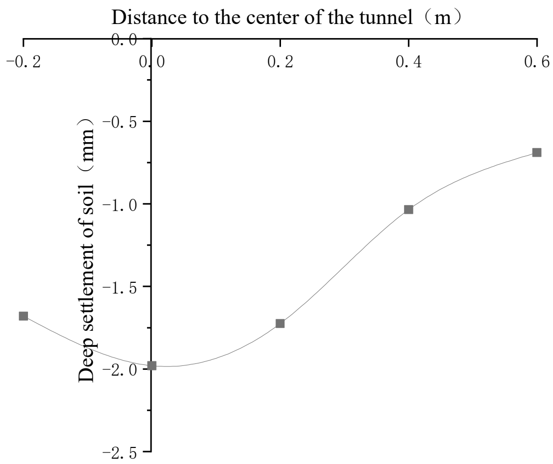

Figure 13. Deep settlement curve of soil (perpendicular to tunnel direction).

It can be seen from Figures 9–11 that: (1) Under the action of ground surcharges, due to the increase of vertical earth pressure, the tunnel has a downward settlement, and the transverse convergence deformation law of the tunnel is basically the same as the vertical deformation of the tunnel, but the numerical value is the opposite, which indicates that the vertical diameter of the tunnel decreases and the transverse diameter increases, resulting in a transverse elliptical deformation. (2) The deformation of the tunnel is the largest just below the ground surcharge. With the distance from the ground surcharge center, the settlement, vertical convergence deformation and transverse convergence deformation of the tunnel are all smaller, and the variation law basically accords with a logistic function. The maximum settlement of tunnel is −0.341 mm, which is converted into actual engineering data by the similarity ratio to be −5.286 mm; The maximum vertical convergence deformation of the tunnel is −0.128 mm, which is converted into actual engineering data of −1.984 mm; The maximum transverse convergence deformation value of the tunnel is 0.118 mm, which is converted into the actual engineering data of 1.829 mm.

It can be seen from Figures 12 and 13 that: (1) the deep settlement of soil is related to the distance of ground surcharge, and the deep settlement of soil on both sides of ground surcharge is basically symmetrically distributed, and the maximum deep settlement of soil parallel to the tunnel direction is −1.852 mm, which is converted into actual engineering data by similarity ratio as −28.706 mm; The maximum deep settlement of soil perpendicular to the tunnel direction is −1.980 mm, which is converted into actual engineering data of −30.690 mm. (2) When the distance from the center of the tunnel is 0.2–0.4 m, the deep settlement of soil decreases by 43.5% parallel to the tunnel and 40.0% perpendicular to the tunnel.

3.2. Analysis of Influencing Factors

3.2.1. Influence of Ground Surcharge on Vertical Convergence Deformation and Settlement of Tunnel

According to working condition 6, when the burial depth of the tunnel is 0.6 m, the settlement and vertical convergence deformation of each measuring point of the tunnel segment under different ground surcharge are as shown in Figures 14 and 15.

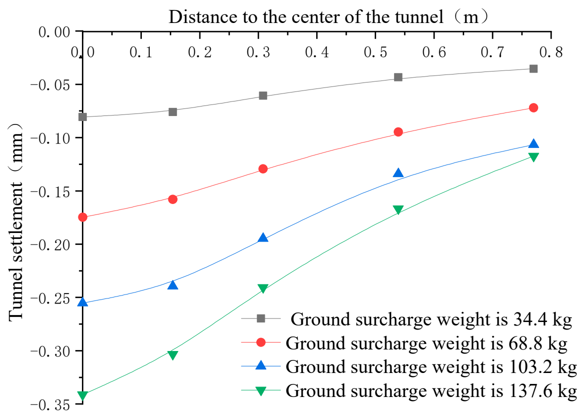

Figure 14. Settlement of each measuring point of tunnel segment under different ground surcharge.

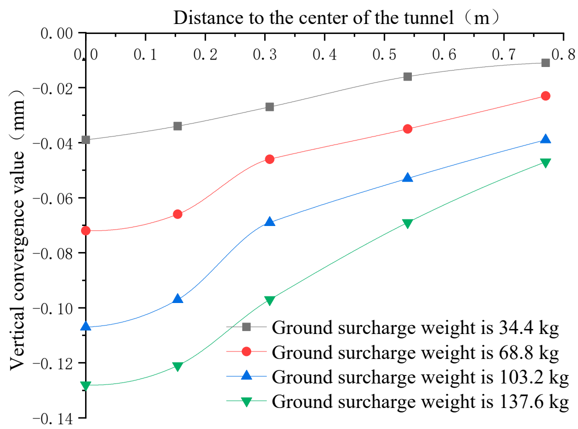

Figure 15. Vertical convergence deformation of each measuring point of tunnel segment under different ground surcharge.

It can be seen from Figures 14 and 15 that the settlement and vertical convergence deformation of the tunnel basically increase linearly with the increase of ground surcharge. The reason is that the ground surcharge value is not large, the convergence deformation and settlement value of the tunnel do not change much under this working condition, and the properties of the tunnel and sand do not change much before and after loading, so the settlement and vertical convergence deformation of the tunnel basically increase linearly during loading.

3.2.2. Influence of Tunnel Depth on Vertical Deformation and Settlement of Tunnel

According to working conditions 5, 6, 7 and 8, when the ground surcharge is 137.6 kg and the tunnel burial depth is 0.5, 0.6, 0.7 and 0.8 m, the settlement and vertical convergence deformation of each measuring point of the tunnel segment under different tunnel burial depths are shown in Figures 16 and 17.

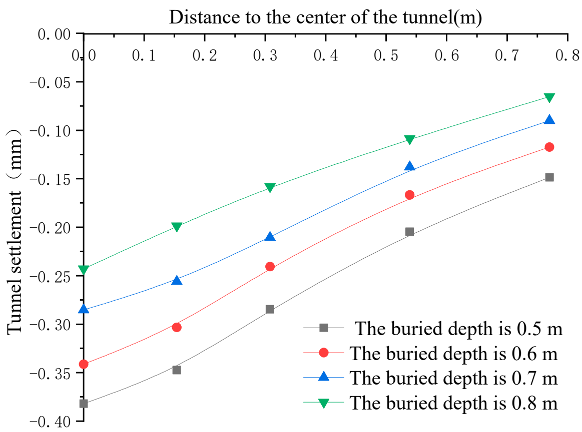

Figure 16. Settlement of each measuring point of tunnel segment at different tunnel depths.

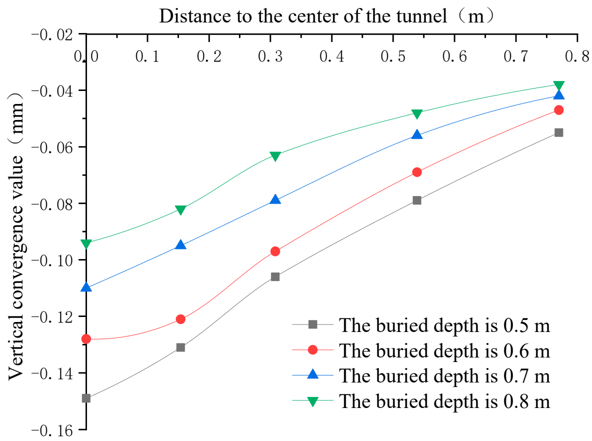

Figure 17. Vertical convergence deformation of each measuring point of tunnel segment at different tunnel depths.

As can be seen in Figures 16 and 17, the magnitude of the stacking load remains constant and as the tunnel burial depth increases and there is a significant reduction in the vertical convergence deformation and settlement of the tunnel. Taking the tunnel segment at the center of the tunnel as an example, when the burial depth of the tunnel changes from 0.5 m to 0.8 m, the vertical convergence deformation decreases from 0.145 mm to 0.094 mm, with a decrease of 35.2%; Settlement decreased from 0.392 mm to 0.243 mm, with a decrease of 38.0%. Therefore, the influence of ground surcharge on the vertical convergence deformation and settlement of tunnel decreases obviously with the increase of buried depth. The test results are basically consistent with the test results in reference [11], but the change trend of the test results is more obvious, which may be related to the different model tunnels used in the test. Wu et al. [11] directly used an iron sheet tube as their tunnel model, while each ring of the tunnel model used in this test is composed of five 67.5° and one 22.5° segment, which is more in line with the actual working conditions.

3.2.3. The Influence of Ground Surcharge Position on Tunnel Transverse Convergence Deformation and Deep Settlement of Soil

(1) Analysis of model test results

According to working conditions 1, 2, 3 and 4, when the burial depth of the tunnel is 0.6 m, the ground surcharge is 137.6 kg, and the eccentric distance of ground surcharge is 0, 0.2, 0.4 and 0.6 m, respectively, the transverse convergence deformation of the center point of the tunnel, the transverse convergence deformation of each measuring point of the tunnel segment, the deep settlement of soil parallel to and perpendicular to the tunnel direction are shown in Figures 18–21.

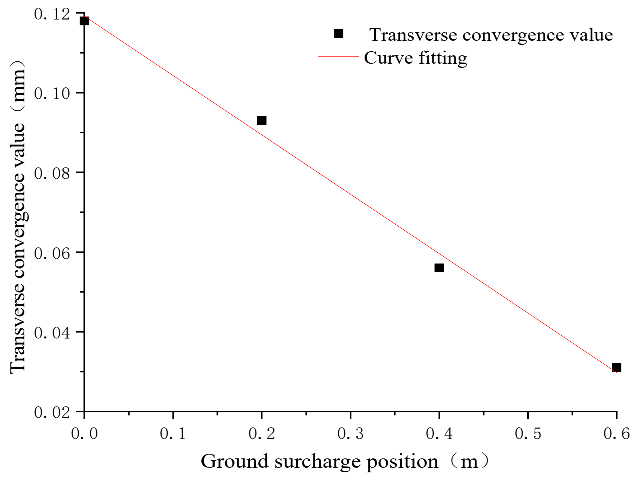

Figure 18. Transverse convergence deformation of tunnel center point under different ground surcharge positions.

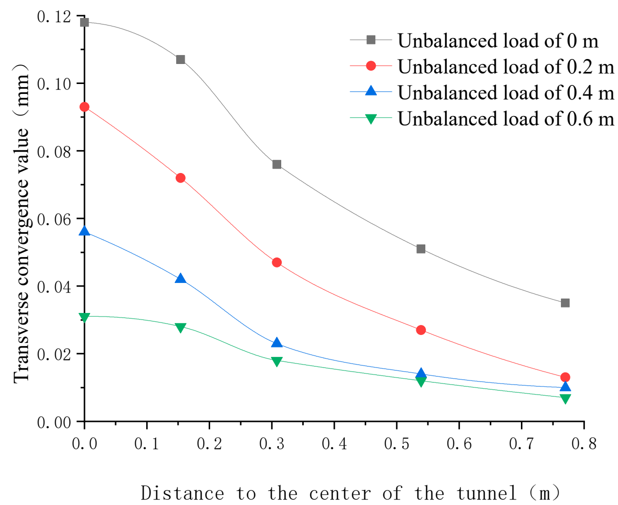

Figure 19. Transverse convergence deformation of each measuring point of tunnel segment under different ground surcharge positions.

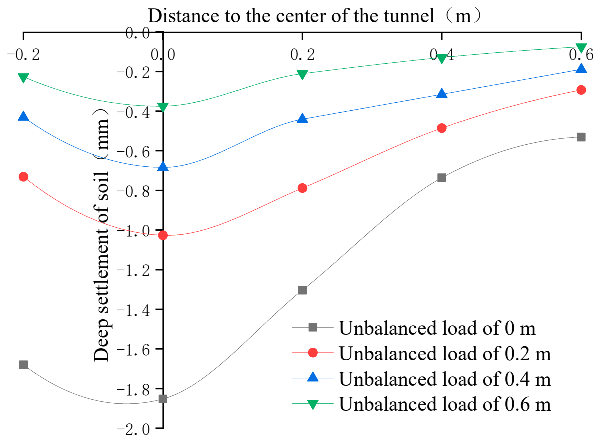

Figure 20. Deep settlement curve of soil parallel to tunnel direction.

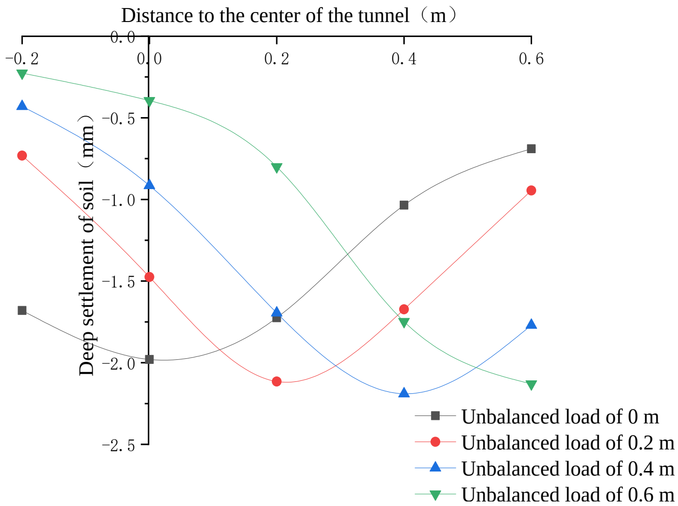

Figure 21. Deep settlement curve of soil perpendicular to tunnel direction.

It can be seen from Figure 18 that the transverse convergence deformation of the tunnel shows a linear downward trend with the increase of the eccentricity distance of the pile load. This is because the distance from the pile load to the measuring point increases during the drift of the pile load, and the influence of the pile load on the tunnel becomes smaller and smaller.

It can be seen from Figure 19 that near the center of the tunnel, the surcharge eccentricity has a great influence on the transverse convergence deformation of each measuring point of the tunnel segment. At the distance away from the center of the tunnel, the transverse convergence deformation of the tunnel segment is very close at different surcharge eccentricity. When the surcharge eccentricity is 0–0.2 m, the surcharge eccentricity distance has the greatest influence on the transverse convergence deformation of each measuring point of the tunnel segment, and then the influence decreases.

It can be seen from Figure 20 that deep soil settlement occurs under the action of ground surcharge, and the deep settlement of soil decreases with the increase of ground surcharge eccentricity. The initial stage of ground surcharge eccentricity has a great influence on the change value of deep settlement of soil, and with the increase of ground surcharge eccentricity, it has less and less influence on the change value of deep settlement of soil, but the curves of deep settlement of soil caused by each eccentric ground surcharge are similar in shape; The settlement of soil below the pile load is the largest, and the relationship between the settlement of soil at different measuring points presents a semi-normal distribution, which is related to the additional stress distribution of soil caused by the pile load.

It can be seen from Figure 21 that with the movement of the pile load, the deep settlement curve of the soil body approximately produces the whole translation in the same direction, and the maximum value is always kept closest to the pile load center, and the settlement on both sides of the pile load center is symmetrically distributed.

(2) Verification of the Boussinesq solution

According to the calculation formula of vertical displacement of soil calculated by the Boussinesq solution, combined with uniformly distributed ground load, the calculation formula of deep settlement of soil is deduced as follows:

$$\omega = \iint \frac{P(1+\mu)}{2\pi E}\left[\frac{z^2}{(x^2+y^2+z^2)^{1.5}} + \frac{2(1-\mu)}{(x^2+y^2+z^2)^{0.5}}\right]dx\,dy \tag{1}$$

where: ω is vertical settlement; μ is poisson's ratio of soil, taking 0.35; E is the elastic modulus of soil, taking 19×10^6 pa; P is the vertical force of ground surcharge on soil.

Using Equation (1), according to the parameters of indoor model tests under working conditions 1, 2, 3 and 4, the results of deep settlement of soil parallel to the tunnel direction and vertical to the tunnel direction are calculated as shown in Figures 22 and 23, in which ω negative values represent downward settlements.

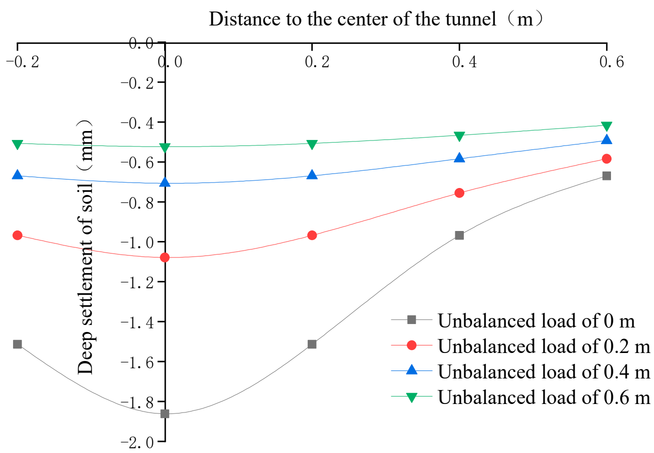

Figure 22. Calculation results of deep settlement of soil parallel to the tunnel direction.

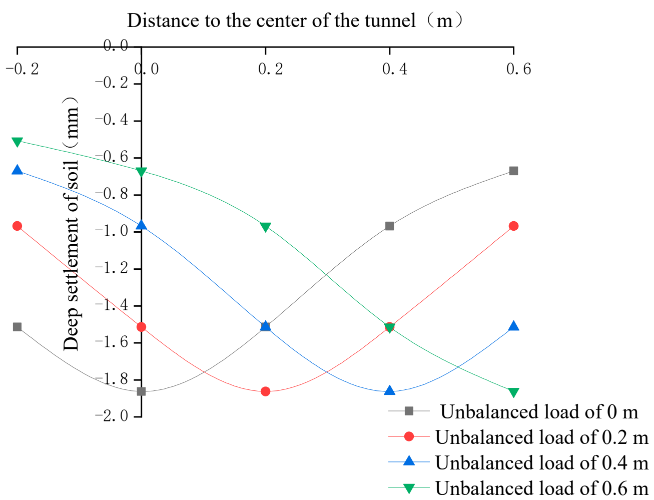

Figure 23. Calculation results of deep settlement of soil perpendicular to the tunnel direction.

Comparing Figure 20 with Figures 21 and 22 with Figure 23, it can be found that the change trend of the model test results is quite consistent with the calculation results of the Boussinesqs solution, which indicates that the deep settlement results of soil obtained from the test are reliable.

Generally, the Poisson's ratio μ of sandy soil is taken in the range of 0.3–0.35, and the elastic modulus E is taken in the range of 10–25 $\times$ 10^6 pa. Taking measurement point 27 as an example, the interaction effect of Poisson's ratio μ and elastic modulus E on settlement ω is shown in Figure 24.

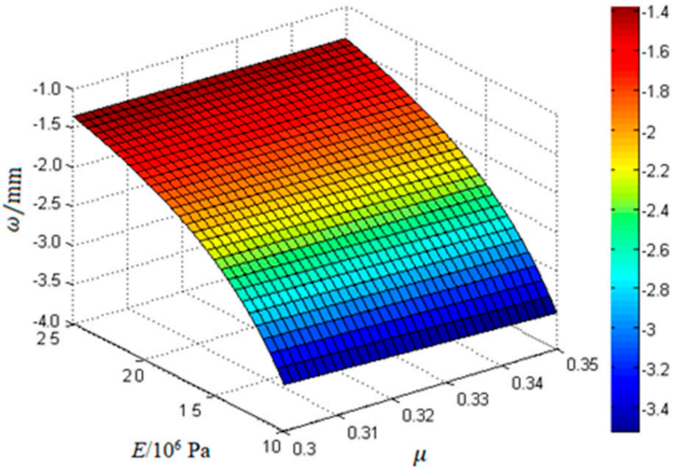

Figure 24. Interaction between Poisson's ratio μ and elastic modulus E on settlement ω.

From Figure 24, it can be seen that with the increase of E, the deep settlement of the soil decreases significantly; with the increase of μ, the deep settlement of the soil increases; compared with both, the effect of E on the deep settlement of the soil is greater than that of μ.

3.2.4. Influence of Different Soil Properties on Vertical Convergence Deformation and Settlement of Tunnel

According to working conditions 6 and 9, when the buried depth of the tunnel is 0.6 m, the influence of different soil quality on the vertical convergence deformation and settlement of the tunnel is shown in Figures 25 and 26. The variation of stress σ with soil layer thickness Z underground surcharge is shown in Figure 27, and the stress σ isolines of different soils are shown in Figure 28.

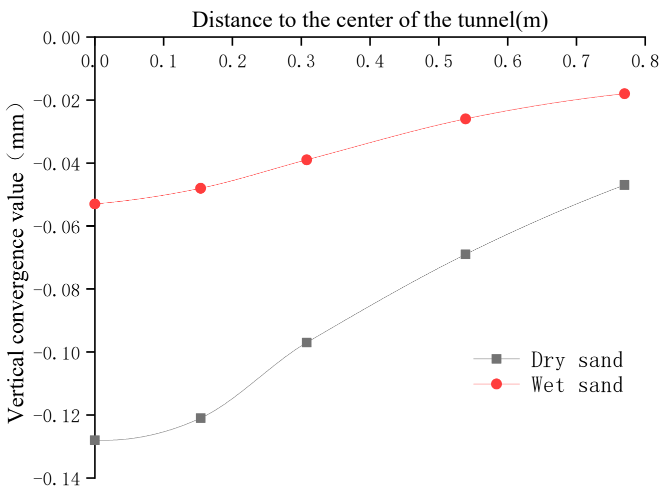

Figure 25. Influence of different soil quality on vertical deformation of tunnel.

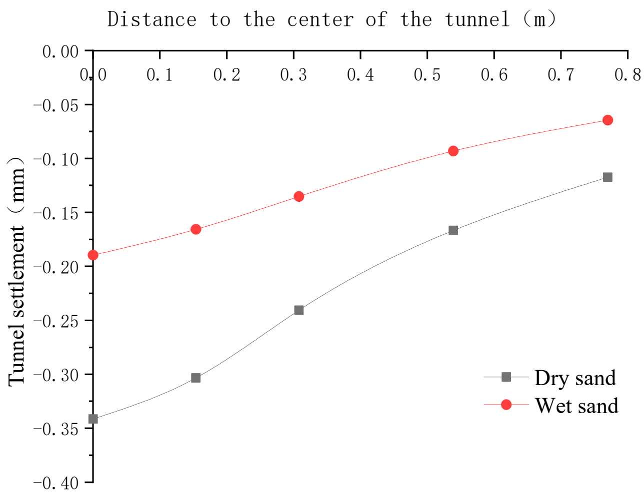

Figure 26. Influence of different soil quality on tunnel settlement.

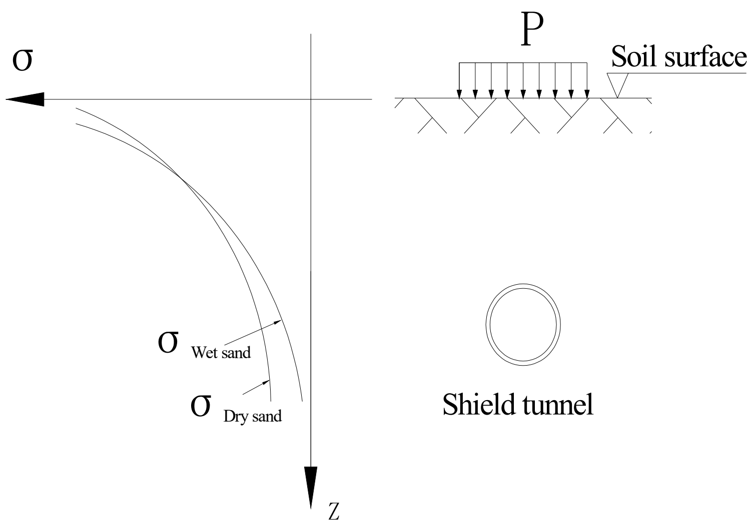

Figure 27. Variation of stress σ with soil layer thickness Z underground surcharge.

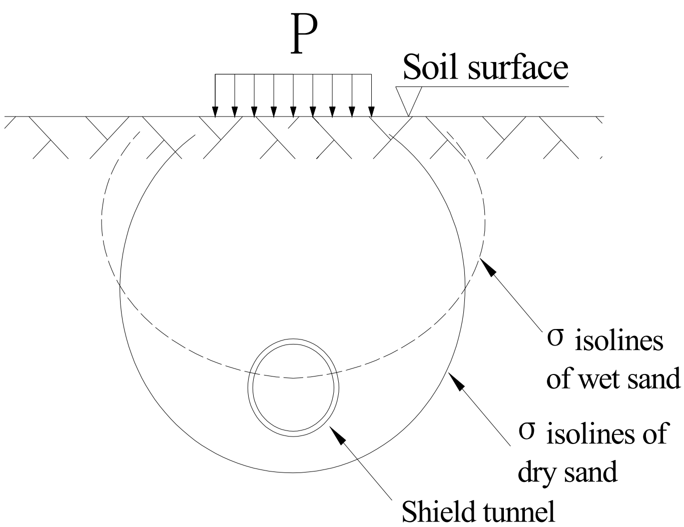

Figure 28. Stress σ isolines of different soils.

It can be seen from Figures 25 and 26 that compared with dry sand, when the test soil used is wet sand, the vertical convergence deformation and settlement of the tunnel are obviously reduced. Taking the vertical deformation at the center of the tunnel as an example, when the test soil is dry sand, the vertical convergence deformation of the tunnel is 0.128 mm, and when the test sand is wet sand, the vertical convergence deformation of the tunnel is 0.053 mm, with a decrease of 58.6%. The tunnel settlement decreased from 0.512 mm to 0.197 mm, with a decrease of 61.5%. The reasons for the above changes may be as follows: (1) When the test soil is wet sand, the sand in the model box is surrounded by an impermeable boundary, and there is excess pore water pressure in the sand, and there is still excess pore water pressure when the soil is damaged. When the excess pore water pressure rises in case of sudden ground surcharge, the effective stress of the soil decreases, and the sand is in a flowing state, which leads to the reduction of additional load on the tunnel, resulting in the reduction of settlement and convergence deformation of the tunnel; (2) As shown in Figures 27 and 28, under the action of ground surcharge, due to the different nature of the soil, the stress σ contours are flat when the soil is wet sand, and the stress σ decreases rapidly with the increase of depth Z. When the soil is dry sand, the stress σ contours are relatively long and lean, and the decrease of stress σ with the increase of depth Z is relatively small, which leads to the settlement and deformation of the tunnel is significantly smaller when the soil is wet sand.

4. Comparative Analysis of Indoor Model Test and Numerical Simulation

4.1. Establishment of 3D Finite Element Model

In this paper, the Midas software is used to establish a finite element three-dimensional numerical model of the influence of ground surcharge on the deformation of adjacent existing shield tunnels. The tunnel segment and soil in the three-dimensional model adopt three-dimensional solid, in which the segment model adopts isotropic elastic model and the soil model adopts isotropic Mohr-Coulomb model. In order to reduce the influence of boundary effect on the calculation results, the horizontal plane size of the model is selected as 40 m $\times$ 57.6 m. The depth dimension of the model varies with the tunnel depth, ranging from 28.45 m to 33.1 m. The upper part of the model simulates the free boundary of the surface, the lower part imposes normal and tangential constraints, and the front, back, left and right boundaries impose normal constraints. The working conditions of three-dimensional finite element numerical model are shown in Table 6, and the finite element model with buried depth of 9.3 m is shown in Figure 29.

Table 6. Working conditions of finite element three-dimensional numerical model.

Test Number	Ground Surcharge Position	Tunnel Buried Depth	Type of Soil
1	Eccentricity 0 m	9.3 m	Sand
2	Eccentricity 3.1 m	9.3 m	Sand
3	Eccentricity 6.2 m	9.3 m	Sand
4	Eccentricity 9.3 m	9.3 m	Sand
5	Eccentricity 0 m	7.75 m	Sand
6	Eccentricity 0 m	9.3 m	Sand
7	Eccentricity 0 m	10.85 m	Sand
8	Eccentricity 0 m	12.4 m	Sand

4.2. Model Calculation Parameters

The sand model parameters are weight 16.2 kN/m^3, Young's modulus 19 MPa, Poisson's ratio 0.29, and internal friction angle 29°. The parameters of shield segment are set according to the geometric parameters of tunnel prototype in Table 2 except elastic modulus. Considering the influence of actual segment joints and bolts, the elastic modulus of segment is reduced by 90% of the values in the table.

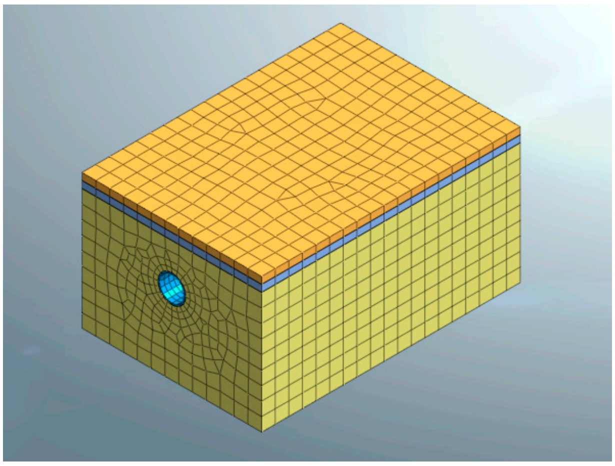

Figure 29. Three-dimensional finite element model.

4.3. Comparative Analysis of Simulation Results and Test Results

The overall settlement trend of the finite element tunnel model is shown in Figure 30, which is basically consistent with the test results.

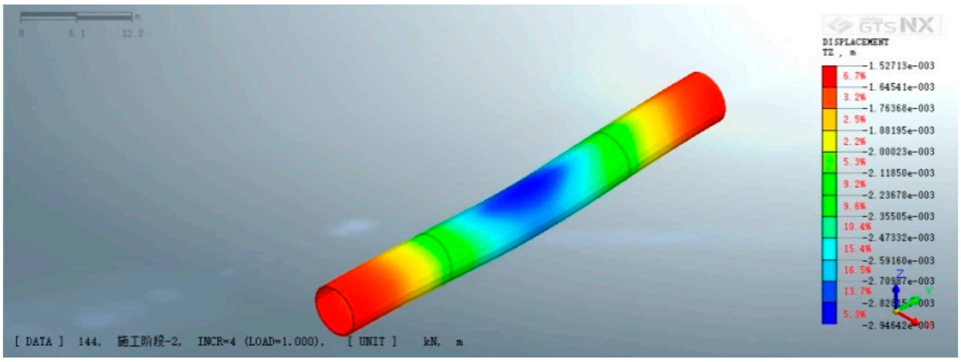

Figure 30. Deformation diagram of tunnel.

The data measured in laboratory tests are converted into actual engineering data by using the similarity ratio, and the obtained data are compared with the finite element simulation results. Although there is a certain gap between the two results, they are certainly of the same order of magnitude. Because the finite element method is often used for qualitative research, a dimensionless comparative study is carried out in this paper.

See Figures 31 and 32 for dimensionless comparison of tunnel settlement and vertical convergence deformation under different ground surcharges. See Figures 33–35 for a dimensionless comparison of tunnel transverse convergence deformation, deep settlement of soil parallel to the tunnel direction and deep settlement of soil perpendicular to the tunnel direction. See Figure 36 for a dimensionless comparison of the vertical convergence deformation of tunnels under different burial depths.

It can be seen from Figure 31 that the tunnel settlement test results and the finite element simulation results are very consistent with each other under different ground surcharge conditions applied at the center of the tunnel.

It can be seen from Figures 32, 33 and 35 that the test results of vertical convergence deformation of tunnel under different stacking loads, transverse convergence deformation of tunnel under different ground surcharge and deep settlement of soil perpendicular to tunnel direction under different stacking loads are in good agreement with the finite element simulation results.

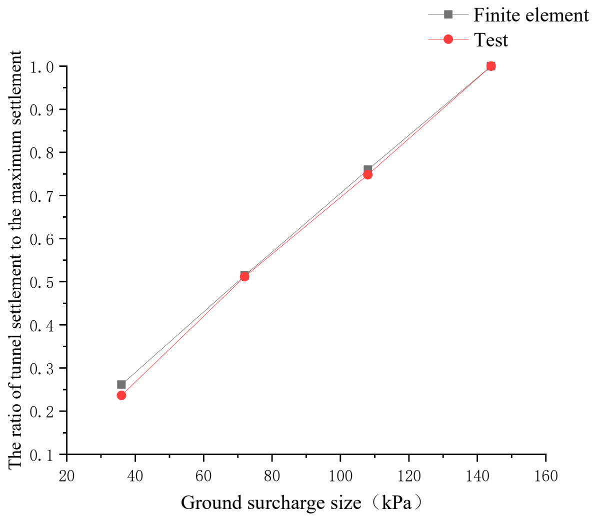

Figure 31. Dimensionless comparison diagram of tunnel settlement under different ground surcharges.

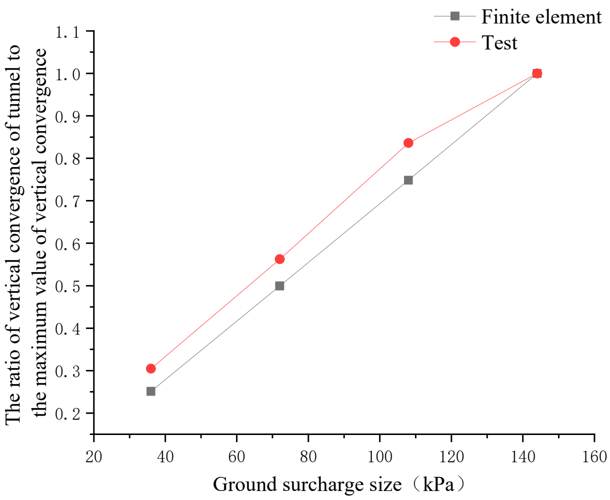

Figure 32. Dimensionless comparison diagram of vertical convergence deformation of tunnel under different ground surcharges.

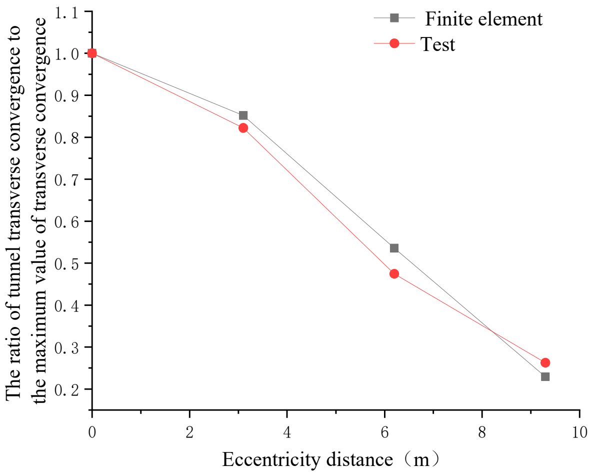

Figure 33. Dimensionless comparison diagram of tunnel transverse convergence deformation at different ground surcharge positions.

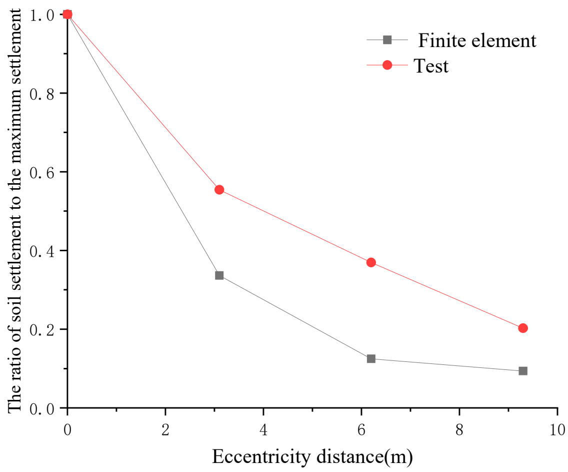

Figure 34. Dimensionless comparison diagram of deep settlement of soil parallel to the tunnel direction.

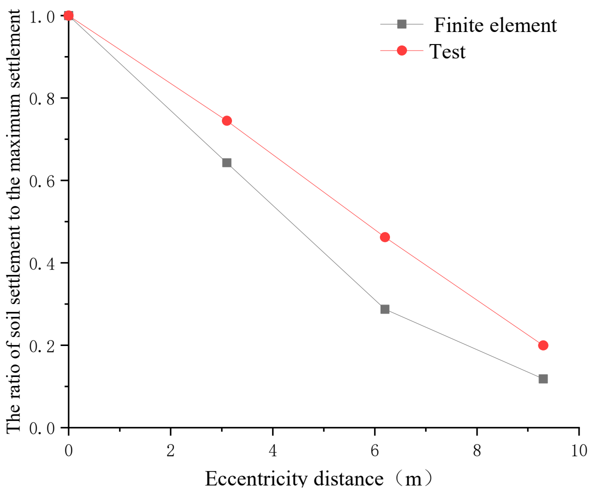

Figure 35. Dimensionless comparison diagram of deep settlement of soil perpendicular to the tunnel direction.

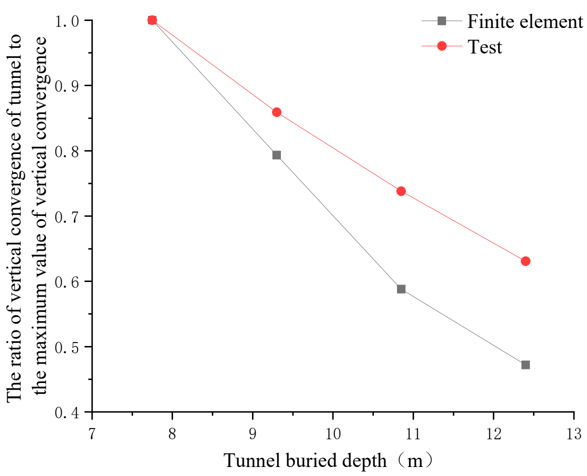

Figure 36. Dimensionless comparison diagram of vertical convergence deformation of the tunnel under different burial depths.

It can be seen from Figures 34 and 36 that the deep settlement of soil parallel to the tunnel direction and the vertical convergence deformation test of tunnel under different burial depths are in good agreement with the finite element simulation, but there is a certain difference between the ratio of test results and the ratio of finite element simulation. Possible reasons are as follows: (1) Due to the site, similarity ratio and economic reasons, the size of the model box should not be too large in the indoor test, which leads to the influence of the boundary effect of the model box on the test, and some errors will be produced when the model test results are placed directly according to the similarity ratio. (2) Although the sand used in the test has been static, the static time is short and the sand is still loose. (3) In the finite element simulation, the segments are continuous without considering the bolts and joints, which is different from the tunnel model used in the indoor model test.

5. Conclusions

(1) The maximum values of tunnel settlement, vertical convergence deformation, transverse convergence deformation and deep settlement of soil all occur at the nearest place to the center of ground surcharge, which is the weakest point of the tunnel under ground surcharge conditions.
(2) When the ground surcharge is the same, the vertical convergence deformation and settlement of the shield tunnel are obviously reduced with the increase of the burial depth of the shield tunnel, which indicates that increasing the burial depth of the shield tunnel can reduce the harm caused by ground surcharges.
(3) Compared with the dry sand, when the test soil is wet sand, the vertical convergence deformation and settlement of the tunnel are significantly reduced, indicating that the nature of the soil has a great impact on the vertical convergence deformation and settlement of the tunnel, and the wet sand is more resistant to the vertical convergence deformation and settlement of the tunnel caused by the ground surcharge than the dry sand.
(4) In calculating the deep settlement of soil caused by surface loading using the Boussinesq solution, the Poisson's ratio μ and the modulus of elasticity E of the soil have a greater influence on the calculation results of the deep settlement of the soil, and the influence of E on the deep settlement of the soil is greater than that of when comparing the two.
(5) The finite element method can simulate well the variation laws of transverse and vertical convergence deformation, tunnel settlement and deep settlement of soil caused by sudden surcharges on the ground. Using less model tests to determine the model and parameters of finite element, and then using finite element to carry out a large number of simulations can improve the research efficiency while ensuring the research accuracy.

Horizontal movement of tunnel was not tested in this model test. There are few kinds of soil used in studying the influence of different soil properties on the vertical convergence deformation and settlement of tunnels. These aspects still need further improvement in future experiments and research.

Author Contributions: Guidance, review and revision, G.W.; model test, S.Z.; analysis, translation, editing and review, P.X. All authors have read and agreed to the published version of the manuscript.

Funding: This research was supported by National Natural Science Foundation of China (Grant No. 51778576).

Institutional Review Board Statement: Not applicable.

Informed Consent Statement: Not applicable.

Data Availability Statement: Not applicable.

Conflicts of Interest: The authors declare no conflict of interest.

References

1. Liu, J.T.; Chen, S.W.; Ye, Z.W. Analysis of disease and structural safety of shield tunnel under accidental surface surcharge. *J. Railw. Eng. Soc.* **2019**, *36*, 67–73.
2. Shao, H.; Huang, H.W.; Zhang, D.M.; Wang, R.L. Case study on repair work for excessively deformed shield tunnel under accidental surface surcharge in soft clay. *Chin. J. Geotech. Eng.* **2016**, *38*, 1036–1043.
3. Lin, Y.G.; Liao, S.M.; Liu, G.B. A discussion of the factors effecting on longitudinal deformation of subway tunnel. *Undergr. Space* **2000**, *20*, 264–267, 289.
4. Lo, K.Y.; Ramsay, J.A. The effect of construction on existing subway tunnels—A case study from Toronto. *Tunn. Undergr. Space Technol.* **1991**, *6*, 287–297. [CrossRef]
5. Xie, J.C.; Wang, J.C.; Huang, W.M. Nonlinear structural analysis on cracking behavior of shield tunnel segment under surface loading. *J. Railw. Sci. Eng.* **2021**, *18*, 162–171.
6. Wei, G.; Hong, W.Q.; Wei, X.J.; Jiang, J.Q. Deformation law and control limit of shield tunnel cross-section under eccentric surcharge load. *J. Cent. South Univ. (Sci. Technol.)* **2020**, *51*, 750–757.
7. Sang, Y.L.; Liu, X.Z.; Zhang, Q. Stiffness analysis and application of segment annular joint based on bolt-concave and convex tenon connection in metro shield tunnel. *Tunn. Constr.* **2020**, *40*, 19–27.
8. Lu, D.Y.; Xu, G.W.; Wang, S.M. Effects of material damage and structural characteristics on tunnel shield during loading and unloading. *J. Southwest Jiaotong Univ.* **2017**, *52*, 1104–1112.
9. Sun, L.W.; Qin, J.S.; Hong, Y.; Wang, L.Z.; Zhao, C.J.; Qin, X. Shield tunnel segment and circumferential joint performance under surface surcharge. *J. Zhejiang Univ. (Eng. Sci.)* **2017**, *51*, 1509–1518.
10. Liu, X.; Zhang, H.L.; Lu, L.; Wang, X.Z. Experimental study on load bearing capacity of shield tunnel structure under overload condition. *Undergr. Eng. Tunn.* **2013**, *4*, 10–15, 59.
11. Wu, Q.; Du, S.J. Model test on influence of ground heaped load on existing shield tunnel structure. *Chin. J. Undergr. Space Eng.* **2014**, *10*, 57–66.
12. Huang, D.W.; Zhou, S.H.; Lai, G.Q.; Feng, Q.S.; Liu, L.Y. Mechanisms and characteristics for deterioration of shield tunnels under surface surcharge. *Chin. J. Geotech. Eng.* **2017**, *39*, 1173–1181.
13. Atkinson, J.H.; Potts, D.M. Stability of a shallow circular tunnel in cohesionless soil. *Geotechnique* **1977**, *27*, 203–215. [CrossRef]
14. Ma, Z.Z.; Luo, Z.H.; Zhang, J.; Xin, H.H. Study on Influence of Ground Surcharge on Deformation of Subway Shield Tunnel. *Mod. Tunn. Technol.* **2018**, *55*, 573–578.
15. Lu, P.Y.; Wang, M.L.; Yang, J.M. Influences of surface surcharge on the deformation of shield tunnel in soft ground area. *Build. Struct.* **2019**, *49*, 999–1003.
16. Wei, G.; Hong, W.Q.; Wei, X.J.; Lin, X.P.; Wang, L.Z. Theoretical calculations of transverse force on shield tunnel caused by eccentric load. *J. Cent. South Univ. (Sci. Technol.)* **2019**, *50*, 1645–1654.
17. Kentaro, Y.; Andrei, V.L.; Daniel, W.W.; Scott, W.S.; Andrew, J.A. Stability of a circular tunnel in cohesive-frictional soil subjected to surcharge loading. *Comput. Geotech.* **2011**, *38*, 504–514.
18. Kentaro, Y.; Andrei, V.L.; Daniel, W.W.; Scott, W.S.; Andrew, J.A. Stability of dual circular tunnels in cohesive-frictional soil subjected to surcharge loading. *Comput. Geotech.* **2013**, *50*, 41–54.
19. Huang, H.W.; Zhang, D.M. Resilience analysis of shield tunnel lining under extreme surcharge: Characterization and field application. *Tunn. Undergr. Space Technol.* **2016**, *51*, 301–312. [CrossRef]
20. Liang, F.Y.; Yuan, Q.; Li, J.P.; Zhang, S.X. Influences of soil characteristics on longitudinal deformation of shield tunnels induced by surface surcharge. *Chin. J. Geotech. Eng.* **2020**, *42*, 63–71.
21. Sun, H.S.; Zhou, T.; Dong, Y.; Chen, Y.D.; Zhang, J.H. Effect of ground surface on the deformation of an existing tunnel. *Chin. J. Undergr. Space Eng.* **2019**, *15*, 900–907, 913.
22. Kang, C.; Mei, G.X.; Liang, R.Z.; Wu, W.B.; Fang, Y.X.; Ke, Z.B. Analysis of the longitudinal deformation of existing shield tunnel induced by temporary surface surcharge. *Rock Soil Mech.* **2018**, *39*, 4605–4616.
23. Mindlin, R.D. Force at a point in the interior of a semiinfinite solid. *Physics* **1936**, *7*, 195–202. [CrossRef]
24. Malt, R.J.; Taylor, R.N. Bored tunneling in the urban environment. In Proceedings of the Fourteenth International Conference on Soil Mechanics and Foundation Engineering, Hamburg, Germany, 6–12 September 1997; pp. 2353–2380.
25. Koyama, Y. Present Status and Technology of Shield Tunneling Method in Japan. *Tunn. Undergr. Space Technol.* **2003**, *18*, 145–159. [CrossRef]
26. Ye, X.Y. Study on the Deformation Test of Subway Tunnel Based on Optical Fiber Sensing Technology. Master's Thesis, Anhui University of Science & Technology, Huainan, China, 2018.